# The modified plasma dispersion function

Cite as: Physics of Fluids B: Plasma Physics **3**, 1835 (1991); https://doi.org/10.1063/1.859653
Submitted: 22 October 1990 • Accepted: 08 April 1991 • Published Online: 04 June 1998

**Danny Summers and Richard M. Thorne**

# The modified plasma dispersion function

Danny Summers
*Department of Mathematics and Statistics, Memorial University of Newfoundland, St. John's, Newfoundland A1C5S7, Canada*

Richard M. Thorne
*Department of Atmospheric Sciences, University of California at Los Angeles, Los Angeles, California 90024-1565*

(Received 22 October 1990; accepted 8 April 1991)

In the linear theory of waves in a hot plasma if the zeroth-order velocity distribution function is taken to be Maxwellian, then there arises a special, complex-valued function of a complex variable $\xi = x + iy$, namely $\mathbf{Z}(\xi)$, known as the plasma dispersion function. In space physics many particle distributions possess a high-energy tail that can be well modeled by a generalized Lorentzian (or kappa) distribution function containing the spectral index $\kappa$. In this paper, as a natural analog to the definition of $\mathbf{Z}(\xi)$, a new special function $\mathbf{Z}_\kappa^*(\xi)$ is defined based on the kappa distribution function. Here, $\mathbf{Z}_\kappa^*(\xi)$ is called the modified plasma dispersion function. For any positive integral value of $\kappa$, $\mathbf{Z}_\kappa^*(\xi)$ is calculated in closed form as a finite series. General properties, including small-argument and large-argument expansions, of $\mathbf{Z}_\kappa^*(\xi)$ are given, and simple explicit forms are given for $\mathbf{Z}_1^*(\xi)$, $\mathbf{Z}_2^*(\xi)$, ..., $\mathbf{Z}_6^*(\xi)$. A comprehensive set of graphs of the real and imaginary parts of $\mathbf{Z}_\kappa^*(\xi)$ is presented. It is demonstrated how the modified plasma dispersion function approaches the plasma dispersion function in the limit as $\kappa \to \infty$, a result to be expected since the (appropriately defined) kappa distribution function formally approaches the Maxwellian as $\kappa \to \infty$. The function $\mathbf{Z}_\kappa^*(\xi)$ is expected to be instrumental in studying microinstabilities in plasmas when the particle distribution function is not only the standard generalized Lorentzian, but also of the Lorentzian type, including *inter alia*, the loss-cone, bi-Lorentzian, and product bi-Lorentzian distributions.

## I. INTRODUCTION

Fried and Conte[1] defined the plasma dispersion function

$$Z(\xi) = \frac{1}{\sqrt{\pi}} \int_{-\infty}^{\infty} \frac{e^{-s^2}}{s - \xi}\, ds, \quad \mathrm{Im}(\xi) > 0 \tag{1}$$

(with a suitable extension for $\mathrm{Im}(\xi) \leqslant 0$ by analytic continuation), where $\xi = x + iy$. The complex-valued function $\mathbf{Z}$ of the complex variable $\xi$ appears in the dispersion equation describing the propagation of waves in a hot plasma when the particle velocity distribution function is linearized about a zeroth-order Maxwellian distribution, e.g.,

$$f_M(v) = (N/\pi^{3/2})(1/\theta^3) e^{-v^2/\theta^2}, \tag{2}$$

where $N$ is the particle number density and $\theta$ is a thermal speed related to the particle temperature $T$ by $\theta = (2T/m)^{1/2}$ where $m$ is the particle mass. Typically, for such a distribution in an unmagnetized plasma and for plasma waves varying as $e^{i(\mathbf{k}\cdot\mathbf{r} - \omega t)}$ where $k$ is the wave number (assumed to be real), and $\omega = \omega_0 + i\gamma$ is the complex wave frequency, $\xi$ takes the form $(\omega_0 + i\gamma)/(k\theta)$. In other situations the variable $\xi$ may take other forms, such as when the given particle distributions have a relative drift, in which case $\xi = (\omega_0 + i\gamma - kv_0)/(k\theta)$ where $v_0$ is the relative drift speed, or when electromagnetic waves propagate parallel to a given magnetic field $B_0$ in which case $\xi = (\omega_0 \pm \Omega_\pm + i\gamma)/(k_\parallel \theta_\parallel)$, where $k_\parallel$ and $\theta_\parallel$ are the wave number and thermal speed parallel to the field and $\Omega_\pm = (eB_0)/(m_\pm c)$ are the ion ( + ) and electron( − ) gyrofrequencies.

The plasma dispersion function (1) defined by Fried and Conte[1] is closely related to the function

$$w(\xi) = \mathbf{Z}(\xi)/(i\sqrt{\pi}) \tag{3}$$

tabulated earlier by Fadeeva and Terent'ev,[2] and to the complex error function erf, where[1,3]

$$\mathbf{Z}(\xi) = i\sqrt{\pi} e^{-\xi^2} [1 + \mathrm{erf}(i\xi)]. \tag{4}$$

While the plasma dispersion function has served many authors (e.g., see Refs. 4–11) as a useful tool in both analytical and numerical studies, the function is strictly only applicable to situations in which the zeroth-order particle distribution function is Maxwellian. In the natural space environment, e.g., planetary magnetospheres, astrophysical plasmas, and the solar wind, plasmas are generally observed to possess a non-Maxwellian high-energy tail.[12–21] A useful distribution function to model such plasmas is the generalized Lorentzian (kappa) distribution

$$f_\kappa(v) = \frac{N}{\pi^{3/2}} \frac{1}{\theta^3} \frac{\Gamma(\kappa + 1)}{\kappa^{3/2}\Gamma(\kappa - 1/2)} \left(1 + \frac{v^2}{\kappa\theta^2}\right)^{-(\kappa+1)}, \tag{5}$$

where $\kappa$ is the spectral index; the thermal speed $\theta$ is related to the particle temperature $T$ by $\theta = [(2\kappa - 3)/\kappa]^{1/2}(T/m)^{1/2}$ when $\kappa > \frac{3}{2}$; $\Gamma$ is the gamma function;[3] and [like distribution (2)] $f_\kappa$ has been normalized so that $\int f_\kappa\, d^3v = N$. Important features of distribution (5) are that, first, at high velocities the distribution obeys an inverse power law [or $f_\kappa \propto (\text{energy})^{-(\kappa+1)}$], and that, sec-

 0899-8221/91/081835-13$02.00  

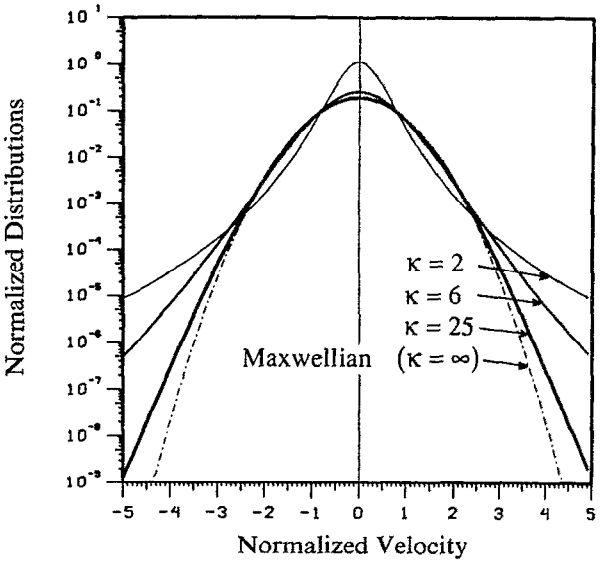


FIG. 1. Comparison of generalized Lorentzian distributions for the spectral index $\kappa = 2$, 6, and 25, with the corresponding Maxwellian distribution ($\kappa = \infty$).

ond, for all velocities, in the limit as the spectral index $\kappa \to \infty$ the distribution approaches the Maxwellian distribution (2). In this sense, the kappa distribution (5) is a generalization of the Maxwellian distribution (2). Vasyliunas[12] appears to have been the first to employ the general form of the kappa distribution (5) and to note its relation to the Maxwellian. Kappa distributions have been used to analyze and interpret spacecraft data on the Earth's magnetospheric plasma sheet,[12-16] the solar wind,[17-19] Jupiter,[20] and Saturn.[21] In practice it is found that many space plasmas can be modeled more effectively by a superposition of kappa distributions than by Maxwellians. In the context of both space and laboratory plasmas Hasegawa *et al.*[22] showed that the equilibrium state of the distribution function for a plasma immersed in superthermal radiation resembles a Lorentzian-type distribution. A direct comparison between the Maxwellian distribution function (2) and the generalized Lorentzian (5) is shown in Fig. 1 for a number of values of $\kappa$. The actual quantities plotted are $(2T/m)^{3/2}f/N$ against $(2T/m)^{-1/2}v$. The Maxwellian and kappa distributions differ substantially in the high-energy tail ($|v/\theta| \gg 1$), but the differences become less significant as $\kappa$ increases.

In Table I we list a number of Lorentzian-type particle distribution functions and their limiting forms as the parameter $\kappa \to \infty$. Motivated by the increasing use of kappa distributions, not only of the standard form (5), but of such forms as given in Table I, and bearing in mind the particular form of (5), we define the function

$$\mathbf{Z}_\kappa^*(\xi) = \frac{1}{\sqrt{\pi}} \frac{\Gamma(\kappa+1)}{\kappa^{3/2}\Gamma(\kappa-1/2)} \times \int_{-\infty}^{\infty} \frac{ds}{(s-\xi)(1+s^2/\kappa)^{\kappa+1}}, \quad \mathrm{Im}(\xi) > 0, \tag{6}$$

which we shall call the *modified plasma dispersion function*, for positive integral values of $\kappa$, with $\xi = x + iy$. For wave problems in which the zeroth-order distribution function is of the generalized Lorentzian type the dispersion equation will typically contain terms involving $\mathbf{Z}_n^*(\xi)$, where $n$ is a positive integer (e.g., see Sec. VI). Accordingly, we expect that a working knowledge of the modified plasma dispersion function will be valuable to theoreticians and experimentalists working on linear plasma instabilities or particle data analysis when the particle distributions contain a substantial high-energy tail component. Parenthetically, we note that definitions (1) and (6) may be regarded as Hilbert transforms of the Maxwellian and kappa distributions.

In the following section we extend definition (6) to values of $\xi$ for which $\mathrm{Im}(\xi) \leqslant 0$, and evaluate $\mathbf{Z}_\kappa^*(\xi)$ in closed form.

## II. EVALUATION OF $\mathbf{Z}_\kappa^*(\xi)$

Let us write (6) in the form,

$$\mathbf{Z}_\kappa^*(\xi) = \frac{1}{\sqrt{\pi}} \frac{\kappa^{(\kappa-1/2)}\Gamma(\kappa+1)}{\Gamma(\kappa-1/2)} F(\xi), \quad \mathrm{Im}(\xi) > 0, \tag{7}$$

where

$$F(\xi) = \int_{-\infty}^{\infty} \frac{\phi(s)}{(s-\xi)}\, ds, \tag{8a}$$

with

$$\phi(s) = (s^2+\kappa)^{-(\kappa+1)}, \tag{8b}$$

and initially we suppose that $\xi \neq \pm i\sqrt{\kappa}$. Then the function $(s-\xi)^{-1}\phi(s)$ has a simple pole at $s = \xi$, a pole of order $\kappa+1$ at $s = i\sqrt{\kappa}$, and a pole of order $\kappa+1$ at $s = -i\sqrt{\kappa}$. We shall use the calculus of residues to evaluate (7) but first we must extend the definition of $\mathbf{Z}_\kappa^*(\xi)$ to the region $\mathrm{Im}(\xi) \leqslant 0$, and we must carefully select the contours of integration in the complex $s$ plane. In order to make the integral $F(\xi)$ continuous across the axis $\mathrm{Im}(\xi) = 0$ we apply the technique of analytic continuation according to the *Landau prescription*. In his pioneering paper in 1946, Landau[26] showed that the correct way to solve the Vlasov equation is as an initial-value problem. Landau's method of choosing the appropriate integration contours has become the basis of analyses of all linear kinetic instabilities of plasma waves. In the present problem, by the Landau prescription (refer to Fig. 2), we set

$$F(\xi) = \begin{cases} \lim\limits_{R\to\infty} \int_{-R}^{R} \dfrac{\phi(s)}{s-\xi}\, ds, & \mathrm{Im}(\xi) > 0, \quad (9) \\ \lim\limits_{\substack{R\to\infty \\ \epsilon\to 0}} \left( \int_{-R}^{\xi-\epsilon} \dfrac{\phi(s)}{s-\xi}\, ds + \int_{\xi+\epsilon}^{R} \dfrac{\phi(s)}{s-\xi}\, ds \right) + \lim\limits_{\epsilon\to 0} \int_{C_2} \dfrac{\phi(s)}{s-\xi}\, ds, & \mathrm{Im}(\xi) = 0, \quad (10) \\ \lim\limits_{R\to\infty} \int_{-R}^{R} \dfrac{\phi(s)}{s-\xi}\, ds + \int_{C_1} \dfrac{\phi(s)}{s-\xi}\, ds, & \mathrm{Im}(\xi) < 0, \quad (11) \end{cases}$$

TABLE I. A selection of Lorentzian-type distributions and their limiting forms as $\kappa \to \infty$.

| "Lorentzian" distribution $f_\kappa$ | Corresponding limiting distribution $\lim_{\kappa\to\infty}(f_\kappa)$ |
|---|---|
| 1. One-dimensional generalized Lorentzian<br>$\frac{N}{\sqrt{\pi}}\frac{1}{\theta}\frac{\Gamma(\kappa+1)}{\kappa^{3/2}\Gamma(\kappa-1/2)}\left(1+\frac{v^2}{\kappa\theta^2}\right)^{-\kappa}$<br>$\theta=[(2\kappa-3)/\kappa]^{1/2}(T/m)^{1/2}$ | One-dimensional Maxwellian<br>$\frac{N}{\sqrt{\pi}}\frac{1}{\theta}e^{-v^2/\theta^2}$<br>$\theta=(2T/m)^{1/2}$ |
| 2. Three-dimensional generalized Lorentzian (Vasyliunas[12])<br>$\frac{N}{\pi^{3/2}}\frac{1}{\theta^3}\frac{\Gamma(\kappa+1)}{\kappa^{3/2}\Gamma(\kappa-1/2)}\left(1+\frac{v^2}{\kappa\theta^2}\right)^{-(\kappa+1)}$<br>$\theta=[(2\kappa-3)/\kappa]^{1/2}(T/m)^{1/2}$ | Three-dimensional Maxwellian<br>$\frac{N}{\pi^{3/2}}\frac{1}{\theta^3}e^{-v^2/\theta^2}$<br>$\theta=(2T/m)^{1/2}$ |
| 3. Bi-Lorentzian<br>$\frac{N}{\pi^{3/2}}\frac{1}{\theta_\perp^2\theta_\parallel}\frac{\Gamma(\kappa+1)}{\kappa^{3/2}\Gamma(\kappa-1/2)}\left(1+\frac{v_\parallel^2}{\kappa\theta_\parallel^2}+\frac{v_\perp^2}{\kappa\theta_\perp^2}\right)^{-(\kappa+1)}$<br>$\theta_\parallel=[(2\kappa-3)/\kappa]^{1/2}(T_\parallel/m)^{1/2},\quad \theta_\perp=[(2\kappa-3)/\kappa]^{1/2}(T_\perp/m)^{1/2}$ | Bi-Maxwellian (Harris[23])<br>$\frac{N}{\pi^{3/2}}\frac{1}{\theta_\perp^2\theta_\parallel}e^{-(v_\parallel^2/\theta_\parallel^2+v_\perp^2/\theta_\perp^2)}$<br>$\theta_\parallel=(2T_\parallel/m)^{1/2},\quad \theta_\perp=(2T_\perp/m)^{1/2}$ |
| 4. Product bi-Lorentzian<br>$\frac{N}{\pi^{3/2}}\frac{1}{\theta_\perp^2\theta_\parallel}\frac{\Gamma(\kappa+1)}{\sqrt{\kappa}\Gamma(\kappa+1/2)}\left(1+\frac{v_\parallel^2}{\kappa\theta_\parallel^2}\right)^{-(\kappa+1)}\left(1+\frac{v_\perp^2}{\kappa\theta_\perp^2}\right)^{-(\kappa+1)}$<br>$\theta_\parallel=[(2\kappa-1)/\kappa]^{1/2}(T_\parallel/m)^{1/2},\quad \theta_\perp=[(2\kappa-2)/\kappa]^{1/2}(T_\perp/m)^{1/2}$ | Bi-Maxwellian (Harris[23])<br>$\frac{N}{\pi^{3/2}}\frac{1}{\theta_\perp^2\theta_\parallel}e^{-(v_\parallel^2/\theta_\parallel^2+v_\perp^2/v_\perp^2)}$<br>$\theta_\parallel=(2T_\parallel/m)^{1/2},\quad \theta_\perp=(2T_\perp/m)^{1/2}$ |
| 5. Lorentzian loss cone<br>$\frac{N}{\pi^{3/2}}\frac{1}{\theta_\perp^2\theta_\parallel}\left(\frac{v_\perp}{\theta_\perp}\right)^{2\sigma}\frac{\Gamma(\kappa+\sigma+1)}{\kappa^{(\sigma+3/2)}\Gamma(\kappa-1/2)\Gamma(\sigma+1)}\left(1+\frac{v_\parallel^2}{\kappa\theta_\parallel^2}+\frac{v_\perp^2}{\kappa\theta_\perp^2}\right)^{-(\kappa+\sigma+1)}$<br>$\theta_\parallel=[(2\kappa-3)/\kappa]^{1/2}(T_\parallel/m)^{1/2},\quad \theta_\perp=(\sigma+1)^{-1/2}[(2\kappa-3)/\kappa]^{1/2}(T_\perp/m)^{1/2}$ | Maxwellian loss cone (Dory *et al.*[24])<br>$\frac{N}{\pi^{3/2}}\frac{1}{\theta_\perp^2\theta_\parallel}\left(\frac{v_\perp}{\theta_\perp}\right)^{2\sigma}\frac{1}{\Gamma(\sigma+1)}e^{-(v_\parallel^2/\theta_\parallel^2+v_\perp^2/\theta_\perp^2)}$<br>$\theta_\parallel=(2T_\parallel/m)^{1/2},\quad \theta_\perp=(\sigma+1)^{-1/2}(2T_\perp/m)^{1/2}$ |
| 6. "Heat-flux" bi-Lorentzian<br>$\left\{1+\gamma_\parallel\left(\frac{v_\parallel}{\theta_\parallel}\right)\left[\frac{2}{3}\left(\frac{v_\parallel}{\theta_\parallel}\right)^2-1\right]+2\gamma_\perp\left(\frac{v_\parallel}{\theta_\parallel}\right)\left[\left(\frac{v_\perp}{\theta_\perp}\right)^2-1\right]\right\}$<br>$\frac{N}{\pi^{3/2}}\frac{1}{\theta_\perp^2\theta_\parallel}\frac{\Gamma(\kappa+1)}{\kappa^{3/2}\Gamma(\kappa-1/2)}\left(1+\frac{v_\parallel^2}{\kappa\theta_\parallel^2}+\frac{v_\perp^2}{\kappa\theta_\perp^2}\right)^{-(\kappa+1)}$<br>$\theta_\parallel=[(2\kappa-3)/\kappa]^{1/2}(T_\parallel/m)^{1/2},\quad \theta_\perp=[(2\kappa-3)/\kappa]^{1/2}(T_\perp/m)^{1/2}$ | "Heat-flux" bi-Maxwellian (Whang[25])<br>$\left\{1+\gamma_\parallel\left(\frac{v_\parallel}{\theta_\parallel}\right)\left[\frac{2}{3}\left(\frac{v_\parallel}{\theta_\parallel}\right)^2-1\right]+2\gamma_\perp\left(\frac{v_\parallel}{\theta_\parallel}\right)\left[\left(\frac{v_\perp}{\theta_\perp}\right)^2-1\right]\right\}$<br>$\frac{N}{\pi^{3/2}}\frac{1}{\theta_\perp^2\theta_\parallel}e^{-(v_\parallel^2/\theta_\parallel^2+v_\perp^2/\theta_\perp^2)}$<br>$\theta_\parallel=(2T_\parallel/m)^{1/2},\quad \theta_\perp=(2T_\perp/m)^{1/2}$ |

where $C_1$ is the semicircular contour in the upper half-plane in each panel of Fig. 2, centered at the origin $s=0$, and of radius $R$, such that $R>\sqrt{\kappa}$ and $R>|\xi|$; $C_2$ is the semicircular contour in Fig. 2 (center panel), with center $s=\xi$, and of radius $\epsilon$; and $C_3$ is the circular contour in Fig. 2 (lower panel), with center $s=\xi$. We calculate the integrals in (9)–(11) by applying the Cauchy residue theorem to the function $(s-\xi)^{-1}\phi(s)$, with the integrations being performed along the respective closed contours specified in Fig. 2 (upper, center, and lower). In each case we find that

$$F(\xi)=2\pi i[\mathrm{Res}(\sqrt{\kappa}i)+\mathrm{Res}(\xi)], \tag{12}$$

where

$$\mathrm{Res}(\sqrt{\kappa}i)=\frac{1}{\kappa!}\frac{d^\kappa}{ds^\kappa}\left(\frac{1}{(s-\xi)(s+\sqrt{\kappa}i)^{\kappa+1}}\right)\Bigg|_{s=\sqrt{\kappa}i} \tag{13}$$

is the residue of the function $(s-\xi)^{-1}\phi(s)$ at $s=\sqrt{\kappa}i$, and

$$\mathrm{Res}(\xi)=\phi(\xi)=(\xi^2+\kappa)^{-(\kappa+1)} \tag{14}$$

is the residue of the function $(s-\xi)^{-1}\phi(s)$ at $s=\xi$. Thus (12) is valid for *all* values of $\xi$ (with the possible exceptions of $\xi=\pm i\sqrt{\kappa}$ to be considered below).

It is worthwhile to verify independently that definitions (9)–(11) do constitute the correct analytic continuation of $F(\xi)$. This may be readily achieved by use of the Plemelj formulas (Muskhelishvili[27]):

$$\lim_{\delta\to 0+}\int_{-\infty}^{\infty}\frac{\phi(s)}{s-\alpha+i\delta}\,ds=P\int_{-\infty}^{\infty}\frac{\phi(s)}{s-\alpha}\,ds-i\pi\phi(\alpha), \tag{15}$$

$$\lim_{\delta\to 0+}\int_{-\infty}^{\infty}\frac{\phi(s)}{s-\alpha-i\delta}\,ds=P\int_{-\infty}^{\infty}\frac{\phi(s)}{s-\alpha}\,ds+i\pi\phi(\alpha), \tag{16}$$

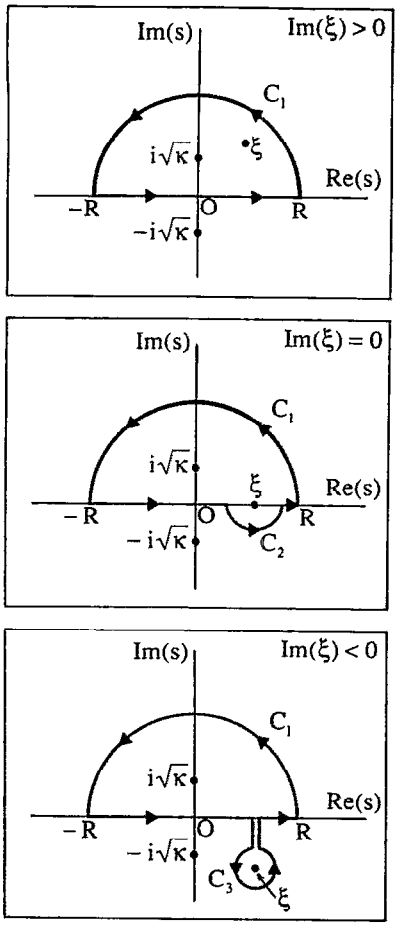


FIG. 2. Landau contours for the evaluation of $\mathbf{Z}_\kappa^*(\xi)$, as given by (6), and its extension by analytic continuation.

where $P$ denotes the Cauchy principal value of the integral. Substitution of $\xi = \alpha + i\delta$ in (9) and application of (16) directly produces (10). Likewise, substitution of $\xi = \alpha - i\delta$ in (11) and application of (15) directly produces (10). Hence, (9) and (11) tend to the same limit (10) as $\mathrm{Im}(\xi) \to 0$. [By definition,

$$P\int_{-\infty}^{\infty} \frac{\phi(s)}{s-\alpha}\,ds = \lim_{\substack{R\to\infty \\ \delta\to 0}} \left( \int_{-R}^{\alpha-\delta} \frac{\phi(s)}{s-\alpha}\,ds + \int_{\alpha+\delta}^{R} \frac{\phi(s)}{s-\alpha}\,ds \right)$$

$$= 2\pi i\,\mathrm{Res}(\sqrt{\kappa}i) + \pi i\,\mathrm{Res}(\alpha)$$

by the Cauchy residue theorem applied to Fig. 2 (center).]

If $\mathrm{Res}(\sqrt{\kappa}i)$ is evaluated from (13) by Leibniz's theorem and the result, together with (14), substituted into (12) and (7), we find

$$\mathbf{Z}_\kappa^*(\xi) = \frac{2\sqrt{\pi}i}{[1+(\xi^2/\kappa)]^{(\kappa+1)}} \frac{\kappa!}{\kappa^{3/2}\Gamma(\kappa-1/2)} \times \left[ 1 - \frac{1}{\kappa!}\frac{1}{2^{\kappa+1}} \left(1 - \frac{i\xi}{\sqrt{\kappa}}\right)^{\kappa+1} \times \sum_{l=0}^{\kappa} \frac{(\kappa+l)!}{l!2^l} \left(1 + \frac{i\xi}{\sqrt{\kappa}}\right)^l \right]. \quad (17)$$

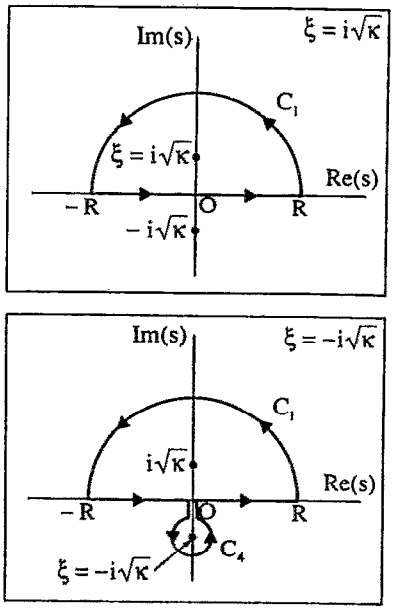


FIG. 3. Landau contours for the evaluation of $\mathbf{Z}_\kappa^*(\xi)$ in the special cases $\xi = \pm i\sqrt{\kappa}$.

Formula (17) is a closed-form expression for $\mathbf{Z}_\kappa^*(\xi)$ for any positive integer $\kappa$, and for all $\xi \neq \pm i\sqrt{\kappa}$. In fact, $\xi = i\sqrt{\kappa}$ is a removable singular point of (17). If $\xi = i\sqrt{\kappa}$ then we can evaluate $\mathbf{Z}_\kappa^*(\xi)$ directly by applying Cauchy's residue theorem to the function $(s - \sqrt{\kappa}i)^{-(\kappa+2)}(s + \sqrt{\kappa}i)^{-(\kappa+1)}$ and the contour in Fig. 3 (upper), with $R \to \infty$. The result is

$$\mathbf{Z}_\kappa^*(i\sqrt{\kappa}) = \frac{(\kappa+1/2)(\kappa-1/2)i}{\kappa^{3/2}(\kappa+1)}. \quad (18)$$

Similarly, for $\xi = -i\sqrt{\kappa}$ integration of $(s - \sqrt{\kappa}i)^{-(\kappa+1)}(s + \sqrt{\kappa}i)^{-(\kappa+2)}$ along the contour in Fig. 3 (lower), in which $C_4$ is a circular contour, center $s = -i\sqrt{\kappa}$, yields

$$\mathbf{Z}_\kappa^*(-i\sqrt{\kappa}) = 0. \quad (19)$$

If the singularity $\xi = i\sqrt{\kappa}$ is removed from (17) then $\mathbf{Z}_\kappa^*(\xi)$ takes the reduced form

$$\mathbf{Z}_\kappa^*(\xi) = -\frac{(\kappa-1/2)}{2\kappa^{3/2}} \frac{\kappa!}{(2\kappa)!} \times \sum_{l=0}^{\kappa} \frac{(\kappa+l)!}{l!} i^{\kappa-l} \left( \frac{2}{(\xi/\sqrt{\kappa}) + i} \right)^{\kappa+1-l}. \quad (20)$$

Result (18) serves as a check on the correctness of formula (20). A further expression for $\mathbf{Z}_\kappa^*(\xi)$ is given in Appendix A.

## III. SPECIFIC FORMS FOR $\mathbf{Z}_1^*(\xi)$, $\mathbf{Z}_2^*(\xi)$,..., $\mathbf{Z}_6^*(\xi)$

In applications of the modified plasma dispersion function to space plasmas we expect the most commonly occurring values of the spectral index $\kappa$ to be $\kappa = 1,2,...,6$. Accordingly, we present here specific forms for $\mathbf{Z}_1^*(\xi)$, $\mathbf{Z}_2^*(\xi)$,..., $\mathbf{Z}_6^*(\xi)$, where $\xi = x + iy$, that are obtainable from formulas (17), (20), or (A3):

$$\mathbf{Z}_1^*(\xi) = -(\xi/2+i)/(\xi+i)^2, \tag{21}$$

$$\mathbf{Z}_2^*(\xi) = -(3\xi^2/4+9\sqrt{2}i\xi/4-4)/(\xi+\sqrt{2}i)^3, \tag{22}$$

$$\mathbf{Z}_3^*(\xi) = -(5\xi^3/6+10\sqrt{3}i\xi^2/3-29\xi/2 - 8\sqrt{3}i)/(\xi+\sqrt{3}i)^4, \tag{23}$$

$$\mathbf{Z}_4^*(\xi) = -(7\xi^4/8+35i\xi^3/4-69\xi^2/2-65i\xi + 256/5)/(\xi+2i)^5, \tag{24}$$

$$\mathbf{Z}_5^*(\xi) = -(9\xi^5/10+27\sqrt{5}i\xi^4/5-67\xi^3-87\sqrt{5}i\xi^2 + 4215\xi/14+640\sqrt{5}i/7)/(\xi+\sqrt{5}i)^6, \tag{25}$$

$$\mathbf{Z}_6^*(\xi) = -(11\xi^6/12+77\sqrt{6}i\xi^5/12-115\xi^4-189\sqrt{6}i\xi^3 + 1093\xi^2+595\sqrt{6}i\xi-6144/7)/(\xi+\sqrt{6}i)^7. \tag{26}$$

Small-argument and large-argument expansions of the plasma dispersion function $\mathbf{Z}(\xi)$ have proved very effective in applications, and even though we have above expressed $\mathbf{Z}_1^*(\xi)$, $\mathbf{Z}_2^*(\xi)$,..., $\mathbf{Z}_6^*(\xi)$ exactly as simple rational functions, we likewise expect expansions of the modified plasma dispersion function for small $\xi$ and large $\xi$ to be useful. Power series expansions in $\xi$ and $1/\xi$ follow readily from (21)–(26). We report these for the convenience of the reader: Power series for $\xi\to 0$:

$$\mathbf{Z}_1^*(\xi) = i(1-2\xi^2+\cdots)-\tfrac{3}{2}\xi(1-\tfrac{5}{3}\xi^2+\cdots),$$

$$\mathbf{Z}_2^*(\xi) = \sqrt{2}i(1-\tfrac{3}{2}\xi^2+\cdots)-\tfrac{15}{8}\xi(1-\tfrac{7}{6}\xi^2+\cdots),$$

$$\mathbf{Z}_3^*(\xi) = \frac{8\sqrt{3}i}{9}(1-\tfrac{4}{3}\xi^2+\cdots)-\tfrac{35}{18}\xi(1-\xi^2+\cdots),$$

$$\mathbf{Z}_4^*(\xi) = (8i/5)(1-\tfrac{5}{4}\xi^2+\cdots)-\tfrac{63}{32}\xi(1-\tfrac{11}{12}\xi^2+\cdots),$$

$$\mathbf{Z}_5^*(\xi) = (128\sqrt{5}i/175)(1-\tfrac{6}{5}\xi^2+\cdots) - \tfrac{99}{50}\xi(1-\tfrac{13}{15}\xi^2+\cdots),$$

$$\mathbf{Z}_6^*(\xi) = (128\sqrt{6}i/189)(1-\tfrac{7}{6}\xi^2+\cdots) - \tfrac{143}{72}\xi(1-\tfrac{5}{6}\xi^2+\cdots).$$

Power series for $|\xi|\to\infty$:

$$\mathbf{Z}_1^*(\xi) = \frac{i}{\xi^4}\left(1-\frac{2}{\xi^2}+\cdots\right) - \frac{1}{2\xi}\left(1+\frac{1}{\xi^2}-\frac{3}{\xi^4}+\cdots\right),$$

$$\mathbf{Z}_2^*(\xi) = \frac{8\sqrt{2}i}{\xi^6}\left(1-\frac{6}{\xi^2}+\cdots\right) - \frac{3}{4\xi}\left(1+\frac{2}{3\xi^2}+\frac{4}{\xi^4}+\cdots\right),$$

$$\mathbf{Z}_3^*(\xi) = \frac{72\sqrt{3}i}{\xi^8}\left(1-\frac{12}{\xi^2}+\cdots\right) - \frac{5}{6\xi}\left(1+\frac{3}{5\xi^2}+\frac{9}{5\xi^4}+\cdots\right),$$

$$\mathbf{Z}_4^*(\xi) = \frac{8192i}{5\xi^{10}}\left(1-\frac{20}{\xi^2}+\cdots\right) - \frac{7}{8\xi}\left(1+\frac{4}{7\xi^2}+\frac{48}{35\xi^4}+\cdots\right),$$

$$\mathbf{Z}_5^*(\xi) = \frac{8}{7}\frac{10^4\sqrt{5}i}{\xi^{12}}\left(1-\frac{30}{\xi^2}+\cdots\right) - \frac{9}{10\xi}\left(1+\frac{5}{9\xi^2}+\frac{25}{21\xi^4}+\cdots\right),$$

$$\mathbf{Z}_6^*(\xi) = \frac{81}{7}\frac{2^{14}\sqrt{6}i}{\xi^{14}}\left(1-\frac{42}{\xi^2}+\cdots\right) - \frac{11}{12\xi}\left(1+\frac{6}{11\xi^2}+\frac{12}{11\xi^4}+\cdots\right).$$

To shed further light on the behavior of the modified plasma dispersion function, we present, in Appendix B, explicit expressions for the real and imaginary parts of the functions $\mathbf{Z}_1^*(\xi)$ and $\mathbf{Z}_2^*(\xi)$. We also calculate their expansions for $x\to 0$ and $x\to\infty$, each with $y$ fixed, and for $y\to 0$ and $y\to\infty$, each with $x$ fixed.

## IV. SOME GENERAL PROPERTIES OF $\mathbf{Z}_\kappa^*(\xi)$

The results in this section are valid for all positive integers $\kappa$:

$$\mathbf{Z}_\kappa^*(0) = \kappa!\sqrt{\pi}i/[\kappa^{3/2}\Gamma(\kappa-1/2)], \tag{27}$$

$$\mathbf{Z}_\kappa^*(\xi) = \frac{\kappa!\sqrt{\pi}i}{\kappa^{3/2}\Gamma(\kappa-1/2)}\frac{1}{[1+(\xi^2/\kappa)]^{\kappa+1}} - \frac{(2\kappa-1)(2\kappa+1)}{2\kappa^2} \times\xi\left[1-\left(\frac{2\kappa+3}{3\kappa}\right)\xi^2+\cdots\right], \quad \xi\to 0, \tag{28}$$

$$= \frac{\kappa!\sqrt{\pi}i}{\kappa^{3/2}\Gamma(\kappa-1/2)}\left[1-\left(\frac{\kappa+1}{\kappa}\right)\xi^2+\cdots\right] - \frac{(2\kappa-1)(2\kappa+1)}{2\kappa^2} \times\xi\left[1-\left(\frac{2\kappa+3}{3\kappa}\right)\xi^2+\cdots\right], \quad \xi\to 0, \tag{29}$$

$$\mathbf{Z}_\kappa^*(\xi) = \frac{\kappa!\sqrt{\pi}i}{\kappa^{3/2}\Gamma(\kappa-1/2)}\frac{1}{[1+(\xi^2/\kappa)]^{\kappa+1}} - \left(\frac{2\kappa-1}{2\kappa}\right)\frac{1}{\xi}\left[1+\left(\frac{\kappa}{2\kappa-1}\right)\frac{1}{\xi^2} + \frac{3\kappa^2}{(2\kappa-1)(2\kappa-3)}\frac{1}{\xi^4}+\cdots\right], \quad |\xi|\to\infty, \tag{30}$$

$$= \frac{\kappa!\kappa^{(\kappa-1/2)}\sqrt{\pi}i}{\Gamma(\kappa-1/2)}\frac{1}{\xi^{2(\kappa+1)}}\left(1-\frac{\kappa(\kappa+1)}{\xi^2}+\cdots\right) - \left(\frac{2\kappa-1}{2\kappa}\right)\frac{1}{\xi}\left[1+\left(\frac{\kappa}{2\kappa-1}\right)\frac{1}{\xi^2} + \frac{3\kappa^2}{(2\kappa-1)(2\kappa-3)}\frac{1}{\xi^4}+\cdots\right], \quad |\xi|\to\infty. \tag{31}$$

Formally, the power series (29) and (31) for $\mathbf{Z}_\kappa^*(\xi)$ are, respectively, convergent for $|\xi|<\sqrt{\kappa}$ and $|\xi|>\sqrt{\kappa}$. Useful expansions for the real and imaginary parts of $\mathbf{Z}_\kappa^*(\xi)$ are easily obtainable from (31), and these are given in Appendix C.

The power series[1] for the plasma dispersion function is

$$\mathbf{Z}(\xi) = \sqrt{\pi} i e^{-\xi^2} - 2\xi\,(1 - \tfrac{2}{3}\xi^2 + \cdots), \quad \xi \to 0, \quad (32)$$

while a version[1] of the asymptotic expansion is

$$\mathbf{Z}(\xi) = \sqrt{\pi} i \sigma e^{-\xi^2} - \frac{1}{\xi}\left(1 + \frac{1}{2\xi^2} + \frac{3}{4\xi^4} + \cdots\right), \quad |\xi| \to \infty \quad (33)$$

where

$$\sigma = \begin{cases} 0, & y > 0, \\ 1, & y = 0, \\ 2, & y < 0. \end{cases}$$

We note that as $\kappa \to \infty$ result (28) for $\mathbf{Z}_\kappa^*(\xi)$ becomes formally identical to result (32)for $\mathbf{Z}(\xi)$, and, likewise, result (30) becomes (33) for $\sigma = 1$. Landau and Cuperman[28] comment on a certain confusion in the literature concerning the correct asymptotic expansion for $\mathbf{Z}(\xi)$.

If we differentiate definition (6) with respect to $\xi$ we can thereby derive the relation

$$\frac{d\mathbf{Z}_\kappa^*(\xi)}{d\xi} = -2\left(1 - \frac{1}{4\kappa^2}\right) - 2\left(\frac{\kappa - 1/2}{\kappa}\right)\left(\frac{\kappa + 1}{\kappa}\right)^{3/2} \times \xi\,\mathbf{Z}_{\kappa+1}^*\left[\left(\frac{\kappa + 1}{\kappa}\right)^{1/2}\xi\right]. \quad (34)$$

Result (34)is useful for replacing the derivative of $\mathbf{Z}_\kappa^*$ by a function of $\mathbf{Z}_{\kappa+1}^*$ if this is desired in a particular problem, or, alternatively, (34)can be used as a recursion formula to calculate $\mathbf{Z}_{\kappa+1}^*$ from $\mathbf{Z}_\kappa^*$. As $\kappa \to \infty$, (34) becomes

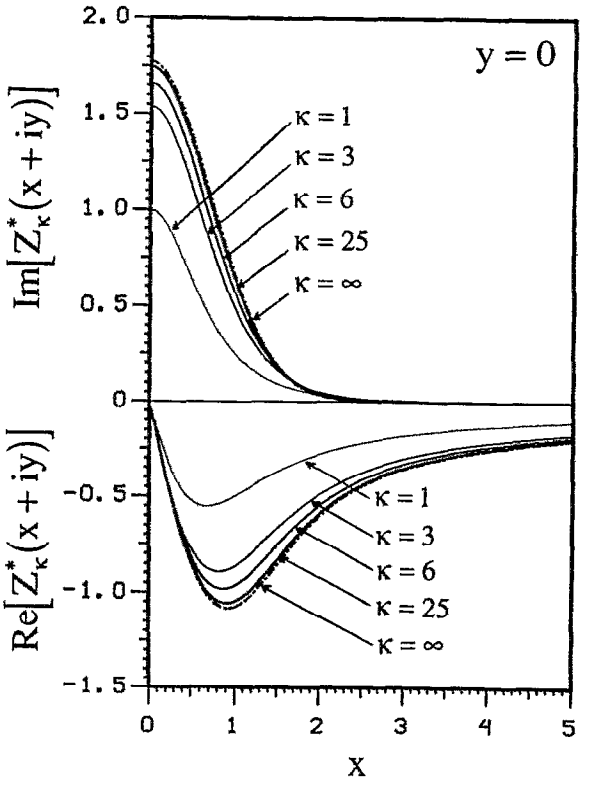


FIG. 4. The imaginary parts (upper curves) and real parts (lower curves) of $\mathbf{Z}_\kappa^*(x + iy)$ for $\kappa = 1$, 3, 6, and 25, each with $y = 0$. Also shown for comparison are the corresponding Maxwellian ($\kappa = \infty$) curves.

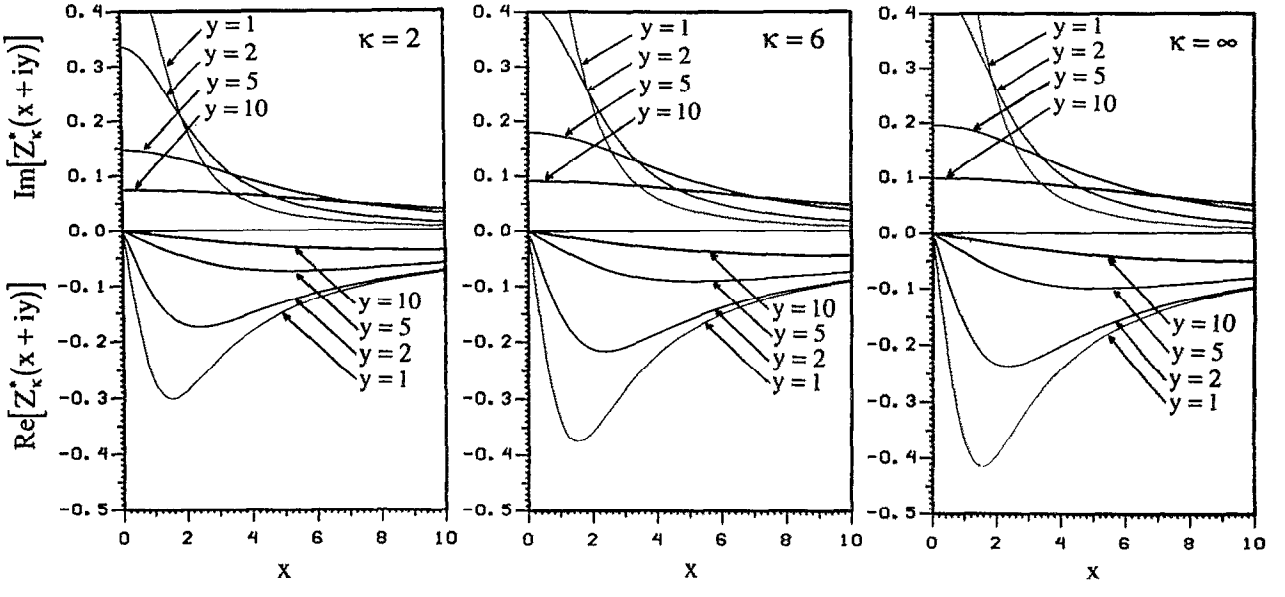


FIG. 5. The imaginary parts (upper curves) and real parts (lower curves) of $\mathbf{Z}_\kappa^*(x + iy)$ for $y = 1$, 2, 5, and 10; and $\kappa = 2$ (left), $\kappa = 6$ (center), and $\kappa = \infty$ (right).

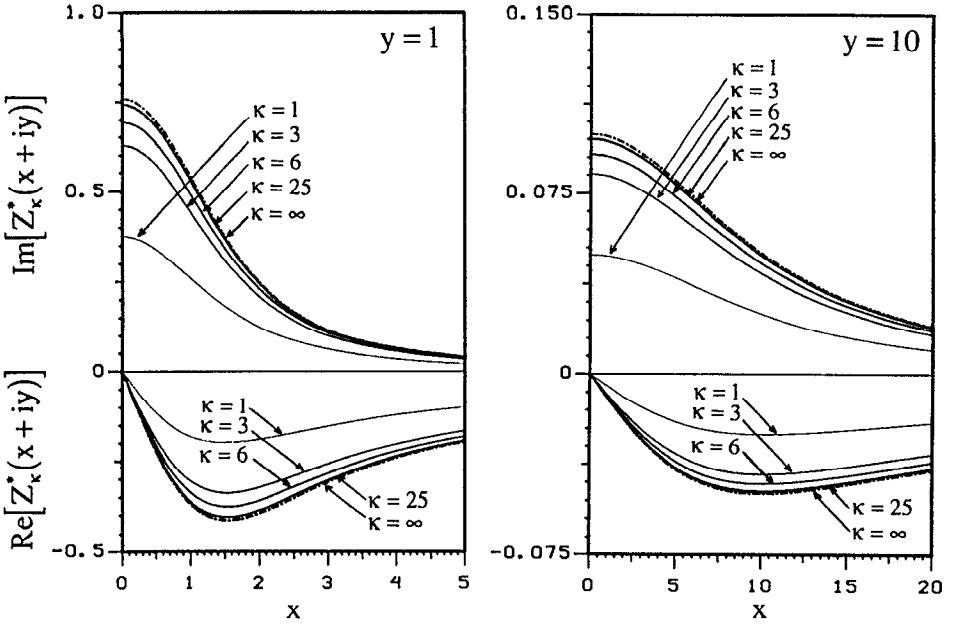


FIG. 6. The imaginary parts (upper curves) and real parts (lower curves) of $\mathbf{Z}_\kappa^*(x+iy)$ for $\kappa = 1$, 3, 6, and 25; and $y = 1$ (left), and $y = 10$ (right). Also shown for comparison are the corresponding Maxwellian ($\kappa = \infty$) curves.

$$\frac{d\mathbf{Z}(\xi)}{d\xi} = -2[1 + \xi\mathbf{Z}(\xi)]. \tag{35}$$

Equation (35) may be regarded as a differential equation characterization[1] of the plasma dispersion function $\mathbf{Z}(\xi)$, subject to $\mathbf{Z}(0) = \sqrt{\pi}i$. The latter condition is realized from (27) by letting $\kappa \to \infty$.

## V. GRAPHICAL RESULTS

To illustrate the behavior of the modified plasma dispersion function $\mathbf{Z}_\kappa^*(\xi)$, with $\xi = x + iy$, and to show its relation to the plasma dispersion function $\mathbf{Z}(\xi)$, we present in Figs. 4–13 graphs of the real and imaginary parts of $\mathbf{Z}_\kappa^*(\xi)$ [and $\mathbf{Z}(\xi)$] as functions of $x$ (with $y$ fixed), and as functions of $y$ (with $x$ fixed). Various values of the spectral index $\kappa$ are chosen.

For $y \geqslant 0$ we find that the behavior of $\mathbf{Z}_\kappa^*(\xi)$ is very similar to that of $\mathbf{Z}(\xi)$. Moreover, as the value of the spectral index $\kappa$ increases, the former functions approach the latter smoothly. Figure 4 shows the variations of the real and imaginary parts of $\mathbf{Z}_\kappa^*(\xi)$ as functions of $x$ in the plane $y = 0$, for $\kappa = 1$, 3, 6, and 25. The corresponding Maxwellian ($\kappa = \infty$) curves, given by Fried and Conte[1] (their Figs. 1 and 2), are also shown. The similarity in the general behavior of $\mathbf{Z}_\kappa^*(\xi)$ and $\mathbf{Z}(\xi)$, even for small values of $\kappa$ (e.g., $\kappa = 1$ and $\kappa = 3$), is clearly evident, as is the trend for $\mathbf{Z}_\kappa^*(\xi)$ to approach $\mathbf{Z}(\xi)$ as $\kappa$ increases. This latter property of the generalized Lorentzian dispersion function has previously been employed[10] to obtain a simple approximation to $\mathbf{Z}(\xi)$. Figure 5 shows the variation of $\mathbf{Z}_\kappa^*(\xi)$ as a function of $x$ in the planes $y = 1$, 2, 5, and 10, for each of the values $\kappa = 2$, 6, and $\infty$. The Maxwellian ($\kappa = \infty$) curves are as given by Fried and Conte[1] (their Figs. 3 and 4). As in Fig. 4, the similarity in behavior of $\mathbf{Z}_\kappa^*(\xi)$ and $\mathbf{Z}(\xi)$, and the role of $\mathbf{Z}(\xi)$ as the limiting form of $\mathbf{Z}_\kappa^*(\xi)$ as $\kappa \to \infty$, are clear. These

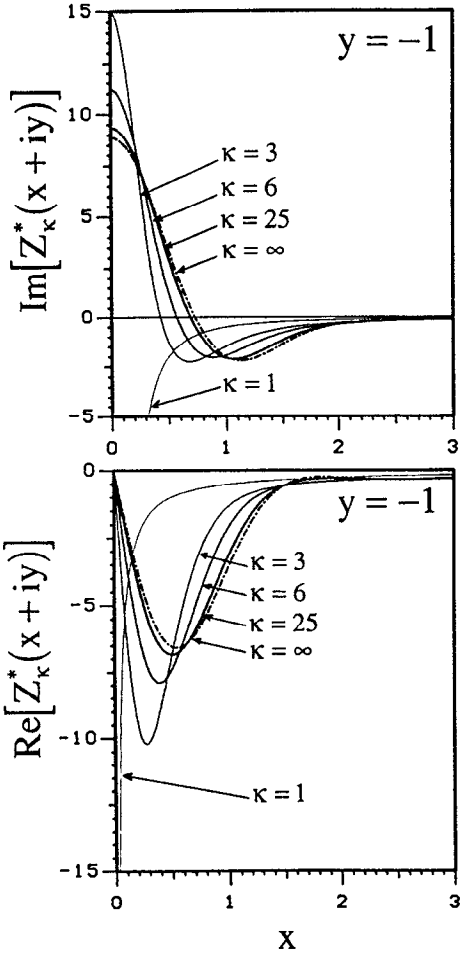


FIG. 7. The imaginary parts (upper curves) and real parts (lower curves) of $\mathbf{Z}_\kappa^*(x+iy)$ for $\kappa = 1$, 3, 6, and 25, each with $y = -1$. Also shown for comparison are the corresponding Maxwellian ($\kappa = \infty$) curves.

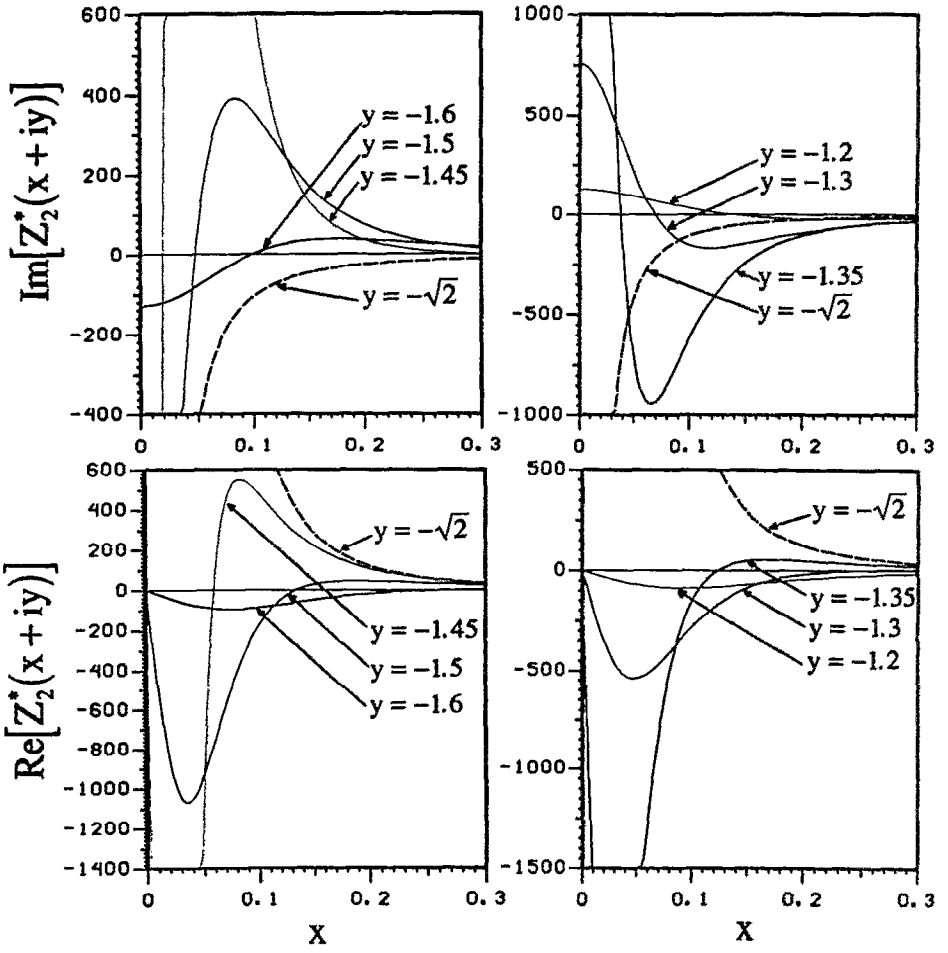


FIG. 8. Imaginary parts (upper curves) and real parts (lower curves) of $\mathbf{Z}_2^*(x+iy)$ for selected values of $y$ to the left (left curves) and to the right (right curves) of $y=-\sqrt{2}$. Also shown are the real and imaginary parts of $\mathbf{Z}_2^*(x-\sqrt{2}i)$.

features are further illustrated in Fig. 6, which is complementary to Fig. 5. Figure 6 shows the variation of $\mathbf{Z}_\kappa^*(\xi)$ as a function of $x$ with $y$ fixed ($y=1$ and $y=10$), and $\kappa$ varying ($\kappa=1$, 3, 6, and 25); again the corresponding variations (for $\kappa=\infty$) of $\mathbf{Z}(\xi)$ are shown for comparison.

Whereas $\mathbf{Z}_\kappa^*(\xi)$ and $\mathbf{Z}(\xi)$ are always "well-behaved" functions for $y\geqslant 0$, both $\mathbf{Z}_\kappa^*(\xi)$ and $\mathbf{Z}(\xi)$ may exhibit erratic behavior for $y<0$. For instance, $\mathbf{Z}_\kappa^*(\xi)$ is discontinuous at $\xi=-i\sqrt{\kappa}$ [formally, $\lim_{\xi\to -i\sqrt{\kappa}}\mathbf{Z}_\kappa^*(\xi)$ does not exist, though $\mathbf{Z}_\kappa^*(-i\sqrt{\kappa})=0$], and in the vicinity of ($x=0$, $y=-\sqrt{\kappa}$) $\mathbf{Z}_\kappa^*(\xi)$ takes on very large values and may exhibit strong oscillations. We show this behavior in Figs. 7–13. It is well known[1] that for ($y<0$ and $|y|>|x|$), $\mathbf{Z}(\xi)$ also has strong oscillations, especially for $|y|\gg 1$. Figure 7 shows $\mathbf{Z}_\kappa^*(\xi)$ as a function of $x$, with $y=-1$, for $\kappa=1$, 3, 6, and 25, together with the Maxwellian case ($\kappa=\infty$), as given by Fried and Conte[1] (their Fig. 7). For $\kappa=3$, 6, and 25, the functions $\mathbf{Z}_\kappa^*(\xi)$ remain bounded for $x\geqslant 0$, and smoothly approach $\mathbf{Z}(\xi)$ as $\kappa$ increases. However, $\lim_{\substack{x\to 0\\ y=-1}}\mathbf{Z}_1^*(\xi)$ does not exist as $\mathbf{Z}_1^*(\xi)$ is unbounded for $x>0$. In fact, from Appendix B, we derive the simple expressions, $\mathrm{Re}[\mathbf{Z}_1^*(x-i)]=-1/(2x)$, and $\mathrm{Im}[\mathbf{Z}_1^*(x-i)]=-1/(2x^2)$. Near $\xi=-\mathrm{i}$ the behavior of $\mathbf{Z}_1^*(\xi)$ is, of course, much different from that of $\mathbf{Z}_\kappa^*(\xi)$ for $\kappa\neq 1$. In Fig. 8 we show the variation of $\mathbf{Z}_2^*(\xi)$ in the vicinity of its point of discontinuity ($x=0, y=-\sqrt{2}$). We show the real and imaginary parts of $\mathbf{Z}_2^*(\xi)$ in the special case $y=-\sqrt{2}$ (namely, from Appendix B, $\mathrm{Re}[\mathbf{Z}_2^*(x-\sqrt{2}i)]=(4-3x^2)/(4x^3)$, and

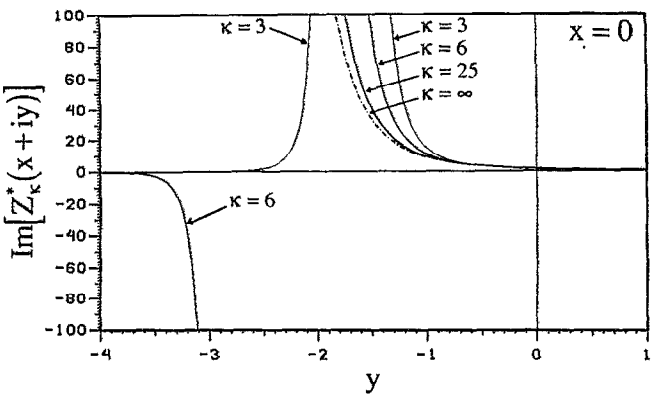


FIG. 9. The imaginary parts of $\mathbf{Z}_\kappa^*(x+iy)$ for $\kappa=3$, 6, and 25, each with $x=0$. Also shown for comparison is the corresponding Maxwellian ($\kappa=\infty$) curve.

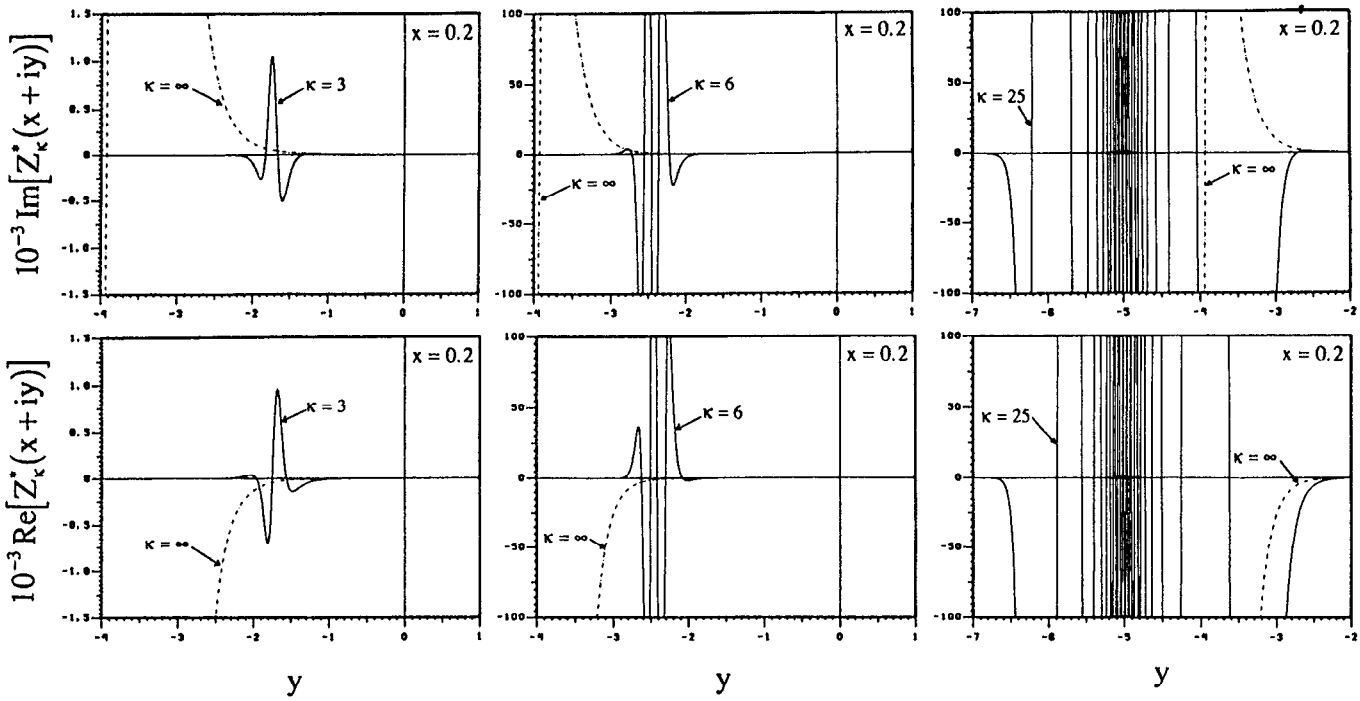


FIG. 10. The imaginary parts (upper curves) and real parts (lower curves) of $\mathbf{Z}^*_\kappa(x+iy)$ for $x=0.2$; and $\kappa=3$ (left), $\kappa=6$ (center), and $\kappa=25$ (right). Also shown for comparison are the Maxwellian ($\kappa=\infty$) curves.

$\mathrm{Im}[\mathbf{Z}^*_2(x-\sqrt{2}i)] = -3\sqrt{2}/(2x^2)$), and also in the planes $y=$ const, just to the left and to the right of $y=-\sqrt{2}$. Both functions $\mathrm{Re}[\mathbf{Z}^*_2(\xi)]$ and $\mathrm{Im}[\mathbf{Z}^*_2(\xi)]$ undergo very large oscillations for $(x\approx 0, y\approx -\sqrt{2})$ which increase without bound as $(x=0,\ y=-\sqrt{2})$ is approached; for $(x=0, y\approx -\sqrt{2})$, $\mathrm{Im}[\mathbf{Z}^*_2(\xi)]$ takes on very large values that again increase arbitrarily as $(x=0,\ y=-\sqrt{2})$ is approached, while $\mathrm{Re}[\mathbf{Z}^*_2(\xi)]=0$. Note that the scale on the vertical axes in Fig. 8 has been greatly extended in comparison to that in previous figures. Though we do not include the curves in our figure, Fried and Conte[1] (their Fig. 9) show the real and imaginary parts of $\mathbf{Z}(\xi)$ for $y=-1.2$, which can be used for comparison with the appropriate curves in Fig. 8. An important difference between $\mathbf{Z}(\xi)$ and $\mathbf{Z}^*_\kappa(\xi)$ is that $\mathbf{Z}(\xi)$ is continuous at the point of discontinuity of $\mathbf{Z}^*_\kappa(\xi)$, i.e., $(x=0, y=-\sqrt{\kappa})$.

Differences in the behavior of $\mathbf{Z}(\xi)$ and $\mathbf{Z}^*_\kappa(\xi)$ for $y<0$ in the planes $x=$ const are further illustrated in Figs. 9–13. In Fig. 9 $\mathrm{Im}[\mathbf{Z}^*_\kappa(\xi)]$ is plotted as a function of $y$, in the plane $x=0$, for $\kappa=3$, 6, 25, and $\infty$; $\mathrm{Re}[\mathbf{Z}^*_\kappa(\xi)]$ vanishes identically when $x=0$. For $\kappa=3$ and $\kappa=6$, Fig. 9 illustrates the nature of $\mathrm{Im}[\mathbf{Z}^*_\kappa(\xi)]$ in the vicinity of the respective points of discontinuity $(x=0, y=-\sqrt{3})$ and $(x=0, y=-\sqrt{6})$. In general when $\kappa$ is odd,

$$\lim_{y\to -\sqrt{\kappa}+}\{\mathrm{Im}[\mathbf{Z}^*_\kappa(0+iy)]\} = \lim_{y\to -\sqrt{\kappa}-}\{\mathrm{Im}[\mathbf{Z}^*_\kappa(0+iy)]\} = +\infty,$$

while when $\kappa$ is even,

$$\lim_{y\to -\sqrt{\kappa}+}\{\mathrm{Im}[\mathbf{Z}^*_\kappa(0+iy)]\} = +\infty$$

and

$$\lim_{y\to -\sqrt{\kappa}-}\{\mathrm{Im}[\mathbf{Z}^*_\kappa(0+iy)]\} = -\infty.$$

For $y\geqslant 0$ the functions $\mathrm{Im}[\mathbf{Z}^*_\kappa(\xi)]$ behave similarly to (and smoothly approach, as $\kappa\to\infty$) $\mathrm{Im}[\mathbf{Z}(\xi)]$. For $y<0$ in general, however, especially for $|y|\gg 1$ and for values of $y$ near $y=-\sqrt{\kappa}$, the functions $\mathrm{Im}[\mathbf{Z}^*_\kappa(\xi)]$ and $\mathrm{Im}[\mathbf{Z}(\xi)]$ display quite different behavior, not least because of the onset of large oscillations in $\mathrm{Im}[\mathbf{Z}(\xi)]$ for $y<0$ (also shown in Fig. 9). Nonetheless, even for $y<0$, we still expect that $\lim_{\kappa\to\infty}[\mathbf{Z}^*_\kappa(\xi)]=\mathbf{Z}(\xi)$, though for an approximate agreement between the values of $\mathbf{Z}^*_\kappa(\xi)$ and $\mathbf{Z}(\xi)$, a very large value of $\kappa$ may have to be taken.

For $x=$ const ($\ll 1$), $\mathbf{Z}^*_\kappa(\xi)$ has oscillations in the vicinity of $y=-\sqrt{\kappa}$ whose amplitude and number increase as $\kappa$ increases (see Fig. 10). Again, for $y<0$ and small values of $\kappa$, $\mathbf{Z}^*_\kappa(\xi)$ and $\mathbf{Z}(\xi)$ behave quite differently. The convergence of $\mathbf{Z}^*_\kappa(\xi)$ to $\mathbf{Z}(\xi)$ as $\kappa\to\infty$ is still not apparent for $\kappa=25$, even though the Lorentzian distribution function when $\kappa=25$ is "close" to the Maxwellian (Fig. 1). Figure 11 is similar to Fig. 10, except that profiles of $\mathbf{Z}^*_\kappa(\xi)$ are shown in the planes $x=0.5$, 1, and 2; with increasing $x$ the aforementioned oscillations become fewer and have smaller amplitudes. In Figs. 12 and 13, which show a selection of curves appearing in Fig. 11 together with the corresponding Max-

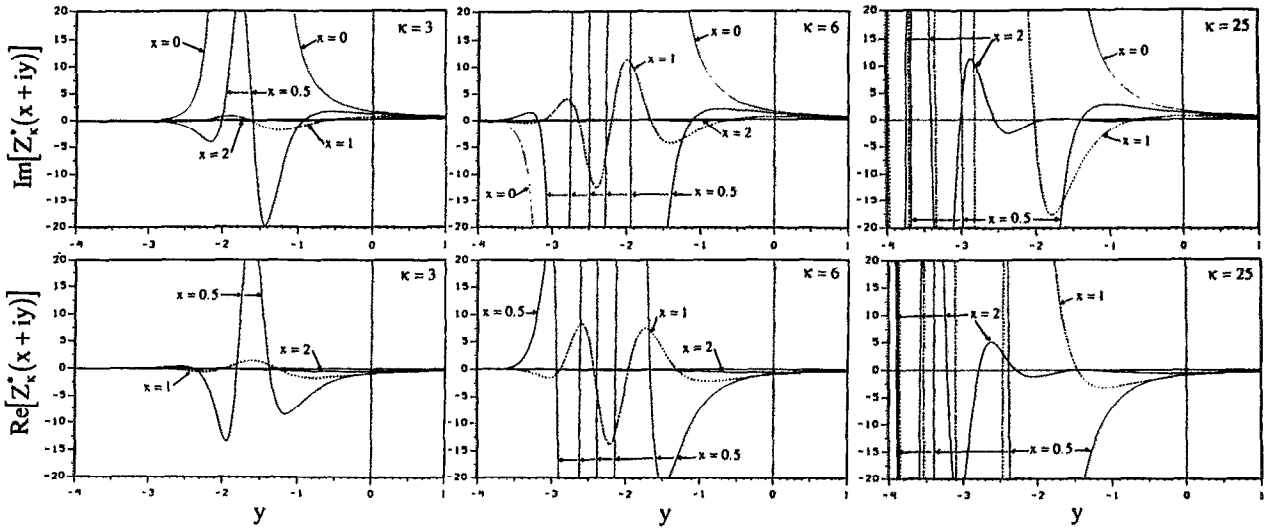


FIG. 11. The imaginary parts (upper curves) and real parts (lower curves) of $\mathbf{Z}_\kappa^*(x+iy)$ for $x = 0, 0.5, 1$, and 2; and $\kappa = 3$ (left), $\kappa = 6$ (center), and $\kappa = 25$ (right). Note that $\mathrm{Re}[\mathbf{Z}_\kappa^*(x+iy)]$ is identically zero for $x = 0$.

wellian profiles, the similarity in general oscillatory behavior of $\mathbf{Z}(\xi)$ and that of $\mathbf{Z}_\kappa^*(\xi)$ for large values of $\kappa$ (e.g., $\kappa = 25$) becomes more apparent but there are still striking differences in behavior between $\mathbf{Z}_\kappa^*(\xi)$ and $\mathbf{Z}(\xi)$ for $y < 0$ (and $|y| \gg 1$), even for $\kappa = 25$.

Evidently, under certain conditions, solutions to the dispersion relation for a given class of waves in a Lorentzian plasma can be expected to differ significantly from the corresponding solutions for a Maxwellian plasma as a result of the qualitative and quantitative differences between the functions $\mathbf{Z}_\kappa^*(\xi)$ and $\mathbf{Z}(\xi)$.[29]

## VI. APPLICATIONS

The primary purpose of this paper is to introduce the modified plasma dispersion function and explore its proper-

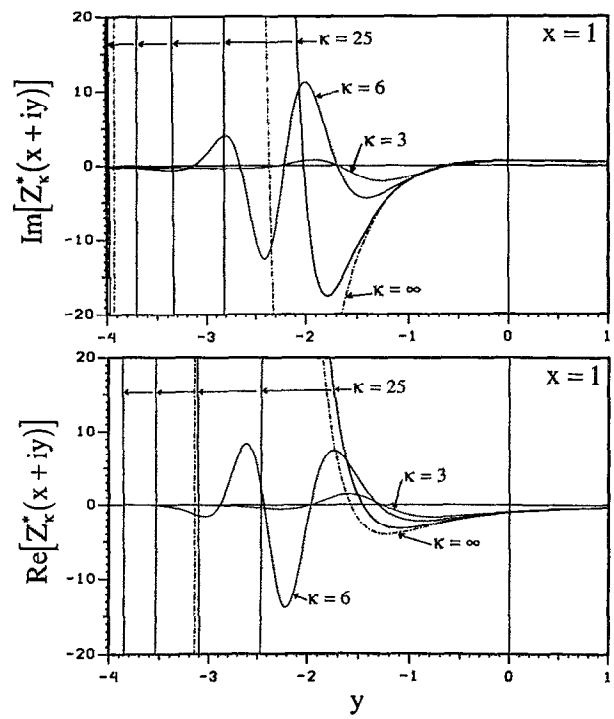


FIG. 12. The imaginary parts (upper curves) and real parts (lower curves) of $\mathbf{Z}_\kappa^*(x+iy)$ for $\kappa = 3$, 6, and 25, each with $x = 1$. Also shown for comparison are the corresponding Maxwellian ($\kappa = \infty$) curves.

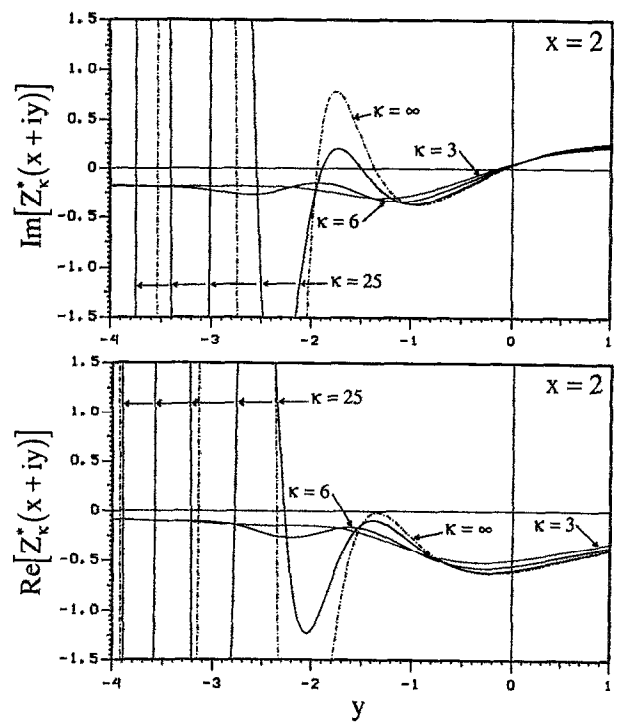


FIG. 13. As Fig. 12, but with $x = 2$.

ties rather than to apply the results to physical problems. However, we shall illustrate precisely how the function arises in two specific cases.

### A. Classical Landau damping of Langmuir waves

Consider longitudinal (Langmuir) waves ($\propto e^{-i\omega t}$) propagating in a hot, isotropic, unmagnetized plasma. Suppose further that we consider electrons only, and that the electrons are modeled by the Maxwellian distribution (2). Then the dispersion equation[11] is

$$1+\frac{2\omega_p^2}{k^2\theta^2}\left[1+\frac{\omega}{k\theta}\mathbf{Z}\left(\frac{\omega}{k\theta}\right)\right]=0, \tag{36}$$

where $\omega=\omega_0+i\gamma$ is the (complex) wave frequency, $k$ is the wave number, $\theta=(2T/m)^{1/2}$ is the electron thermal speed, and $\omega_p=(4\pi Ne^2/m)^{1/2}$ is the electron plasma frequency. If the electrons are modeled by the kappa distribution (5), the corresponding dispersion equation is

$$1+\frac{2\omega_p^2}{k^2\theta^2}\left[1-\frac{1}{2\kappa}+\frac{\omega}{k\theta}\mathbf{Z}_\kappa^*\left(\frac{\omega}{k\theta}\right)\right]=0, \tag{37}$$

where $\theta=[(2\kappa-3)/\kappa]^{1/2}(T/m)^{1/2}$.

We consider detailed solutions to Eqs. (36) and (37), as well as including the ion contribution, in an accompanying paper.[29] An important finding is that the kappa distribution can produce markedly enhanced damping of electron plasma waves in comparison to the results for the Maxwellian distribution in the physically interesting regime of long wavelength, namely $k\lambda_D<1$, where $\lambda_D=(T/m)^{1/2}/\omega_p$ is the electron Debye length.

### B. Electromagnetic (R mode and L mode) waves propagating parallel to a magnetic field in a hot plasma

The dispersion equation[4,5] for circularly polarized electromagnetic waves ($\propto e^{-i\omega t}$) propagating parallel to a uniform magnetic field in a spatially homogeneous plasma consisting of ions ( + ) and electrons ( − ), each species of which is modeled by a bi-Maxwellian distribution, (Table I, 3, right) is

$$1=\frac{\omega^2}{k^2c^2}+\sum_{+,-}\frac{\omega_{p\pm}^2}{k^2c^2}\left\{\frac{\omega}{k\theta_\parallel^{\pm}}\mathbf{Z}\left(\frac{\omega\pm\Omega_\pm}{k\theta_\parallel^{\pm}}\right)-A^{\pm}\left[1+\left(\frac{\omega\pm\Omega_\pm}{k\theta_\parallel^{\pm}}\right)\mathbf{Z}\left(\frac{\omega\pm\Omega_\pm}{k\theta_\parallel^{\pm}}\right)\right]\right\}, \tag{38}$$

where $\omega$ and $k$ are as defined above in Sec. VI A; $c$ is the speed of light; $\omega_{p\pm}$ are the plasma frequencies, $\Omega_\pm$ are the gyrofrequencies, $\theta_\parallel^{\pm}$ are the parallel thermal speeds, and $A^{\pm}=1-(T_\perp^{\pm}/T_\parallel^{\pm})$ are the temperature anisotropies. In Eq. (38) the right-hand (R mode) and left-hand (L mode) waves correspond to selecting the respective combinations $\{\omega+\Omega_+,\omega-\Omega_-\}$ and $\{\omega-\Omega_+,\omega+\Omega_-\}$.

If both ions and electrons are modeled by a bi-Lorentzian distribution (Table I, 3, left), the dispersion equation corresponding to (38) is

$$1=\frac{\omega^2}{k^2c^2}+\sum_{+,-}\frac{\omega_{p\pm}^2}{k^2c^2}\left(\frac{\omega}{k\theta_\parallel^{\pm}}\left(\frac{\kappa}{\kappa-\frac{3}{2}}\right)\left(\frac{\kappa-1}{\kappa}\right)^{3/2}\times\mathbf{Z}_{\kappa-1}^*\left[\sqrt{\frac{\kappa-1}{\kappa}}\left(\frac{\omega\pm\Omega_\pm}{k\theta_\parallel^{\pm}}\right)\right]-A^{\pm}\left\{1+\left(\frac{\kappa-1}{\kappa-\frac{3}{2}}\right)\sqrt{\frac{\kappa-1}{\kappa}}\left(\frac{\omega\pm\Omega_\pm}{k\theta_\parallel^{\pm}}\right)\times\mathbf{Z}_{\kappa-1}^*\left[\sqrt{\frac{\kappa-1}{\kappa}}\left(\frac{\omega\pm\Omega_\pm}{k\theta_\parallel^{\pm}}\right)\right]\right\}\right). \tag{39}$$

A form equivalent to (39) was given by Abraham-Shrauner and Feldman.[17] Equation (39) has a number of interesting applications in space physics, though we do not discuss solutions to this equation here.

## VII. COMMENTS

We have introduced a new special function $\mathbf{Z}_\kappa^*(\xi)$, with $\xi=\kappa+iy$, which we call the modified plasma dispersion function, based on the generalized Lorentzian (kappa) particle distribution function. Our definition of the new function is analogous to the definition[1] of the plasma dispersion function $\mathbf{Z}(\xi)$, which is based on the Maxwellian distribution. While $\mathbf{Z}(\xi)$ and $\mathbf{Z}_\kappa^*(\xi)$ are qualitatively similar for $y\geqslant 0$, there can be substantial differences in the absolute value of the two functions for $y\geqslant 0$ especially for small values of the spectral index $\kappa$. When $y<0$, the behavior of $\mathbf{Z}_\kappa^*(\xi)$ can be dramatically different from that of $\mathbf{Z}(\xi)$. This can lead to significant differences between the dispersive properties of plasma waves in a generalized Lorentzian plasma and a Maxwellian plasma. Since it is now well established that many space plasmas can be modeled by kappa distributions, we expect that $\mathbf{Z}_\kappa^*(\xi)$ should be a useful tool in the analysis of microinstabilities in space plasmas. Moreover, $\mathbf{Z}_\kappa^*(\xi)$ is easier to deal with than $\mathbf{Z}(\xi)$, both from analytical and numerical points of view. The evaluation of $\mathbf{Z}_\kappa^*(\xi)$ in closed form, and the derivation of the expansions and general properties of $\mathbf{Z}_\kappa^*(\xi)$, are straightforward, and, indeed, some of the results in this paper can be readily derived by means of computer symbolic algebra. Notwithstanding this, $\mathbf{Z}_\kappa^*(\xi)$ itself can provide a powerful means of analyzing wave propagation in Lorentzian-type plasmas, as exemplified in our first application[29] of the new function to the classical problem of Landau damping. In fact, in an analysis of the problem which is more thorough than has been possible before [say, by using $\mathbf{Z}(\xi)$], we are even able, for instance, to produce exact analytical solutions for Langmuir oscillations in a Lorentzian plasma in the case $\kappa=2$. In future studies we intend to use $\mathbf{Z}_\kappa^*(\xi)$ to treat microinstabilities in magnetized plasmas driven by particle beams (drifts), and velocity-space anisotropies, e.g., temperature anisotropies or loss-cone effects. Because of the aforementioned differences between $\mathbf{Z}(\xi)$ and $\mathbf{Z}_\kappa^*(\xi)$, the growth (or damping) rate of a particular wave mode in a generalized Lorentzian plasma can be significantly different from that in a Maxwellian plasma, particularly when the resonant particles that give rise to the growth (or damping) of the wave may have speeds that greatly exceed the thermal speed.[29]

## ACKNOWLEDGMENTS

We thank Song Xue and Louise Lee for assistance in construction of the figures, and Robert Strangeway for use of a computer code for evaluating the plasma dispersion function $\mathbf{Z}(x+iy)$.

This work was funded in part by NASA Grant No. NAGW 1639 and by NSF Grant No. ATM 87-18108. D.S. acknowledges support from the Natural Sciences and Engineering Research Council of Canada under Operating Grant A-0621.

## APPENDIX A: AN ALTERNATIVE FORMULA TO (17) AND (20) FOR $Z_\kappa^*(\xi)$

From residue theory it is straightforward to derive the result

$$\int_{-\infty}^{\infty} \frac{ds}{(s-\xi)(s^2+a^2)} = \frac{-\pi}{a(\xi+ia)} = \mathcal{J}(a), \quad \text{(A1)}$$

where $a$ is some positive parameter. By repeated differentiation under the integral sign with respect to $a$, it then follows that

$$\int_{-\infty}^{\infty} \frac{ds}{(s-\xi)(s^2+a^2)^{\kappa+1}} = \frac{(-1)^\kappa}{\kappa!} D^\kappa \mathcal{J}(a), \quad \text{(A2)}$$

where $D \equiv (1/2a)(d/da)$, and $\kappa$ is a positive integer. Thus, from (7), (8), and (A2) we derive the following further expression for $\mathbf{Z}_\kappa^*(\xi)$:

$$\mathbf{Z}_\kappa^*(\xi) = \frac{(-1)^\kappa}{\sqrt{\pi}} \frac{\kappa^{(\kappa-1/2)}}{\Gamma(\kappa-1/2)} D^\kappa \mathcal{J}(a) \,|_{a=\sqrt{\kappa}}. \quad \text{(A3)}$$

## APPENDIX B: EXPLICIT EXPRESSIONS AND EXPANSIONS FOR $Z_1^*(\xi)$ AND $Z_2^*(\xi)$

Explicit expressions and expansions for $\mathbf{Z}_1^*(\xi)$ are listed below and in Table II:

$$\mathrm{Re}[\mathbf{Z}_1^*(x+iy)] = \frac{-x[x^2+(y+1)(y+3)]}{2[x^2+(y+1)^2]^2}, \quad \text{(B1)}$$

$$\mathrm{Im}[\mathbf{Z}_1^*(x+iy)] = \frac{x^2y+(y+1)^2(y+2)}{2[x^2+(y+1)^2]^2}. \quad \text{(B2)}$$

Explicit expressions and expansions for $\mathbf{Z}_2^*(\xi)$ are listed below and in Table III;

$$\mathrm{Re}[\mathbf{Z}_2^*(x+iy)] = \frac{\left(\frac{3}{4}x^2-\frac{3}{4}y^2-\frac{9}{4}\sqrt{2}y-4\right)\left[3x(y+\sqrt{2})^2-x^3\right]+\left(\frac{3}{2}xy+\frac{9}{4}\sqrt{2}x\right)\left[(y+\sqrt{2})^3-3x^2(y+\sqrt{2})\right]}{[x^2+(y+\sqrt{2})^2]^3}, \quad \text{(B3)}$$

$$\mathrm{Im}[\mathbf{Z}_2^*(x+iy)] = \frac{\left(\frac{3}{4}xy+\frac{9}{4}\sqrt{2}x\right)\left[3x(y+\sqrt{2})^2-x^3\right]+\left(\frac{3}{4}x^2-\frac{3}{4}y^2-\frac{9}{4}\sqrt{2}y-4\right)\left[3x^2(y+\sqrt{2})-(y+\sqrt{2})^3\right]}{[x^2+(y+\sqrt{2})^2]^3}. \quad \text{(B4)}$$

TABLE II. Expansions for $\mathbf{Z}_1^*(\xi)$.

| | $\mathrm{Re}[\mathbf{Z}_1^*(x+iy)]$ | $\mathrm{Im}[\mathbf{Z}_1^*(x+iy)]$ |
|---|---|---|
| $y$ fixed, $x\to 0$ | $-\frac{(y+3)x}{2(y+1)^3}+\frac{(y+5)x^3}{2(y+1)^5}+\cdots$ | $\frac{(y+2)}{2(y+1)^2}-\frac{(y+4)x^2}{2(y+1)^4}+\cdots$ |
| $y$ fixed, $x\to\infty$ | $-\frac{1}{2x}+\frac{(y+1)(y-1)}{2x^3}+\cdots$ | $\frac{y}{2x^2}-\frac{(y+1)^2(y-2)}{2x^4}+\cdots$ |
| $x$ fixed, $y\to 0$ | $-\frac{x(x^2+3)}{2(x^2+1)^2}+\frac{4xy}{(x^2+1)^3}+\cdots$ | $\frac{1}{(x^2+1)^2}+\frac{(x^4+6x^2-3)y}{2(x^2+1)^3}+\cdots$ |
| $x$ fixed, $y\to\infty$ | $-\frac{x}{2y^2}+\frac{x(x^2+3)}{2y^4}+\cdots$ | $\frac{1}{2y}-\frac{(x^2+1)}{2y^3}+\cdots$ |

TABLE III. Expansions for $\mathbf{Z}_2^*(\xi)$.

| | $\mathrm{Re}[\mathbf{Z}_2^*(x+iy)]$ | $\mathrm{Im}[\mathbf{Z}_2^*(x+iy)]$ |
|---|---|---|
| $y$ fixed, $x\to 0$ | $-\frac{3(y^2+4\sqrt{2}y+10)x}{4(y+\sqrt{2})^4}+\frac{(3y^2+18\sqrt{2}y+70)x^3}{4(y+\sqrt{2})^6}+\cdots$ | $\frac{(3y^2+9\sqrt{2}y+16)}{4(y+\sqrt{2})^3}-\frac{3(y^2+5\sqrt{2}y+16)x^2}{4(y+\sqrt{2})^5}+\cdots$ |
| $y$ fixed, $x\to\infty$ | $-\frac{3}{4x}+\frac{(3y^2-2)}{4x^3}+\cdots$ | $\frac{3y}{4x^2}-\frac{3y(y+\sqrt{2})(y-\sqrt{2})}{4x^4}+\cdots$ |
| $x$ fixed, $y\to 0$ | $-\frac{x(3x^4+20x^2+60)}{4(x^2+2)^3}+\frac{48\sqrt{2}xy}{(x^2+2)^4}+\cdots$ | $\frac{8\sqrt{2}}{(x^2+2)^3}+\frac{3(x^6+10x^4+60x^2-40)y}{4(x^2+2)^4}+\cdots$ |
| $x$ fixed, $y\to\infty$ | $-\frac{3x}{4y^2}+\frac{3x(x^2+2)}{4y^4}+\cdots$ | $\frac{3}{4y}-\frac{(3x^2+2)}{4y^3}+\cdots$ |

TABLE IV. Expansions for $\mathbf{Z}_\kappa^*(\xi)$ derived from Eq. (31).

| $\kappa > 2$ | $\mathrm{Re}[\mathbf{Z}_\kappa^*(x+iy)]$ | $\mathrm{Im}[\mathbf{Z}_\kappa^*(x+iy)]$ |
|---|---|---|
| $y$ fixed, $x \to \infty$ | $-\frac{(2\kappa-1)}{2\kappa x}+\frac{[(2\kappa-1)y^2-\kappa]}{2\kappa x^3}+\cdots$ | $\frac{(2\kappa-1)y}{2\kappa x^2}+\frac{y[3\kappa-(2\kappa-1)y^2]}{2\kappa x^4}+\cdots$ |
| $x$ fixed, $y \to \infty$ | $-\frac{(2\kappa-1)x}{2\kappa y^2}+\frac{x[3\kappa+(2\kappa-1)x^2]}{2\kappa y^4}+\cdots$ | $\frac{(2\kappa-1)}{2\kappa y}-\frac{[\kappa+(2\kappa-1)x^2]}{2\kappa y^3}+\cdots$ |

## APPENDIX C: EXPANSIONS FOR $\mathbf{Z}_\kappa^*(\xi)$ DERIVED FROM (31)

See Table IV for the expansions for $\mathbf{Z}_\kappa^*(\xi)$ derived from (31).


[1]B. D. Fried and S. D. Conte, *The Plasma Dispersion Function* (Academic, New York, 1961).
[2]V. N. Fadeeva and N. M. Terent'ev, *Tables of Values of the Probability Integral for Complex Arguments* (GITTL, Moscow, 1954).
[3]N. Abramowitz and I. A. Stegun, *Handbook of Mathematical Functions* (Dover, New York, 1965).
[4]J. E. Scharer and A. W. Trivelpiece, Phys. Fluids **10**, 591 (1967).
[5]J. M. Cornwall and M. Schulz, J. Geophys. Res. **76**, 7791 (1971).
[6]J. M. Kindel and C. F. Kennel, J. Geophys. Res. **76**, 3055 (1971).
[7]S. Cuperman, L. Gomberoff, and A. Sternlieb, J. Plasma Phys. **13**, 259 (1975).
[8]D. D. Sentman, J. P. Edmiston, and L. A. Frank, J. Geophys. Res. **86**, 7487 (1981).
[9]M. P. Leubner and A. F. Viñas, J. Geophys. Res. **91**, 13366 (1986).
[10]P. A. Robinson and D. L. Newman, J. Plasma Phys. **40**, 553 (1988).
[11]D. G. Swanson, *Plasma Waves* (Academic, San Diego, 1989).
[12]V. M. Vasyliunas, J. Geophys. Res. **73**, 2839 (1968).
[13]A. T. Y. Lui and S. M. Krimigis, Geophys. Res. Lett. **8**, 527 (1981).
[14]A. T. Y. Lui and S. M. Krimigis, Geophys. Res. Lett. **10**, 13 (1983).
[15]D. J. Williams, D. G. Mitchell, and S. P. Christon, Geophys. Res. Lett. **15**, 303 (1988).
[16]S. P. Christon, D. G. Mitchell, D. J. Williams, L. A. Frank, C. Y. Huang, and T. E. Eastman, J. Geophys. Res. **93**, 2562 (1988).
[17]B. Abraham-Shrauner and W. C. Feldman, J. Plasma Phys. **17**, 123 (1977).
[18]B. Abraham-Shrauner, J. R. Asbridge, S. J. Bame, and W. C. Feldman, J. Geophys. Res. **84**, 553 (1979).
[19]J. T. Gosling, J. R. Asbridge, S. J. Bame, W. C. Feldman, R. D. Zwickl, G. Paschman, N. Sckopke, and R. J. Hynds, J. Geophys. Res. **86**, 547 (1981).
[20]M. P. Leubner, J. Geophys. Res. **87**, 6335 (1982).
[21]T. P. Armstrong, M. T. Paonessa, E. V. Bell II, and S. M. Krimigis, J. Geophys. Res. **88**, 8893 (1983).
[22]A. Hasegawa, K. Mima, and M. Duong-van, Phys. Rev. Lett. **54**, 2608 (1985).
[23]E. G. Harris, J. Nucl. Energy C **2**, 138 (1961).
[24]R. A. Dory, G. E. Guest, and E. G. Harris, Phys. Rev. Lett. **14**, 131 (1965).
[25]Y. C. Whang, J. Geophys. Res. **76**, 7503 (1971).
[26]L. D. Landau, J. Phys. (U.S.S.R.) **10**, 25 (1946).
[27]N. I. Muskhelishvili, *Singular Integral Equations* (Noordhoff, Groningen, 1953).
[28]R. W. Landau and S. Cuperman, J. Plasma Phys. **6**, 495 (1971).
[29]R. M. Thorne and D. Summers, Phys. Fluids B **3**, 2117 (1991).